

# Location Division Multiple Access for Near-Field Communications

Zidong Wu and Linglong Dai

Department of Electronic Engineering, Tsinghua University,  
Beijing National Research Center for Information Science and Technology (BNRist), Beijing 100084, China  
Email: wuzd19@mails.tsinghua.edu.cn, daill@tsinghua.edu.cn

**Abstract**—Spatial division multiple access (SDMA) is essential to improve the spectrum efficiency for multi-user multiple-input multiple-output (MIMO) communications. The classical SDMA for massive MIMO with hybrid precoding heavily relies on the angular orthogonality in the far field to distinguish multiple users at different angles, which fails to fully exploit spatial resources in the distance domain. With dramatically increasing number of antennas, extremely large-scale antenna array (ELAA) introduces additional resolution in the distance domain in the near field. In this paper, we propose the concept of location division multiple access (LDMA) to provide a new possibility to enhance spectrum efficiency. The key idea is to exploit extra spatial resources in the distance domain to serve different users at different locations (determined by angles and distances) in the near field. Specifically, the asymptotic orthogonality of beam focusing vectors in the distance domain is proved, which reveals that near-field beam focusing is able to focus signals on specific locations to mitigate inter-user interferences. Simulation results verify the superiority of the proposed LDMA over classical SDMA in different scenarios.

**Index Terms**—Spatial division multiple access (SDMA), massive MIMO, Extremely large-scale antenna array (ELAA), near-field, location division multiple access (LDMA).

## I. INTRODUCTION

Massive multiple-input multiple-output (MIMO), which employs dozens or hundreds of antennas at the base station (BS), has become the key enabler to increasing spectrum efficiency by orders of magnitude in the fifth-generation (5G) networks. Spatial division multiple access (SDMA) is essential to simultaneously serve multiple user equipments (UEs) to achieve spectrum efficiency enhancement in massive MIMO systems [1]. Moreover, to meet the requirement of the 10-fold increase in spectrum efficiency for 6G, massive MIMO is evolving into the extremely large-scale antenna array (ELAA) equipped with thousands of antennas [2].

For the widely adopted hybrid precoding architecture in massive MIMO and ELAA systems, SDMA is usually realized by the joint design of analog and digital precoding. Since the analog precoding is realized by phase shifters, the constant modulus constraints of phase shifters impose difficulties on designs of analog precoding, which is the main challenge for SDMA in hybrid precoding schemes [3].

Recently, owing to the characteristics of the channel, much research has focused on employing beam steering vectors to construct the analog precoder [3]. By exploiting the sparsity of massive MIMO channels at high frequencies, beam steering vectors corresponding to directional beams can be directly

utilized to focus the signal energy in desired directions to serve UEs. Meanwhile, owing to the angular asymptotic orthogonality of directional beams as the number of antennas tends to infinity, the received signal power could be maximized while inter-user interferences could be naturally eliminated [4]. Following this insight, a practical two-stage multi-user precoding method was proposed in [5]. In the first stage, the analog precoder is selected from a predefined beam-steering codebook, such as discrete Fourier transform (DFT) codebooks, to maximize the received signal power and partially alleviate inter-user interferences. Then, the digital precoder is designed to further eliminate the remained interferences.

Following such methods, to further enhance the spectrum efficiency, communication systems commonly rely on the high-cost way of increasing antennas to generate thinner beams, where analog precoding could eliminate interferences more thoroughly. Besides enlarging arrays only, this paper investigates a new possibility to boost the spectrum efficiency.

Inspired by near-field communications recently investigated in [6], we find that the extra resolution in the distance domain brought by near-field beams could be exploited to enhance spectrum efficiency. Specifically, the transition from massive MIMO to ELAA implies that the classical far-field *planar-wave* propagation model is not accurate anymore because of the significantly increased array aperture [6]. To precisely characterize the channel, near-field *spherical-wave* propagation model has to be adopted, where the communications are referred to near-field communications. Owing to the different electromagnetic wave propagation models, unlike the far-field steering beams focusing signal energy on a certain angle, near-field beams are capable of focusing signal energy on a specific location [7], which could be leveraged to mitigate interferences from UEs that can not be distinguished by far-field beams.

In this paper, the concept of location division multiple access (LDMA) is proposed, which aims to exploit extra spatial resources in the distance domain to enhance spectrum efficiency. Specifically, the LDMA communication scheme is proposed, which exploits the energy-focusing property of near-field beams to serve different UEs located at different angles and different distances, i.e. locations, to improve the system performance. Then, similar to the asymptotic orthogonality of far-field beams in the angular domain, the asymptotic orthogonality of near-field beams in the distance domain is investigated. Moreover, by virtue of the asymptotic orthogo-

nality of near-field beams, the performance analysis is provided to reveal the asymptotic optimality of LDMA schemes. Simulation results are provided to verify the superiority of the LDMA scheme compared with classical SDMA schemes.

## II. SYSTEM MODEL

### A. System Model

We consider a time division duplexing (TDD) narrow-band ELAA single-cell millimeter-wave (mmWave) communication scenario. The BS is equipped with an  $N$ -antenna uniform linear array (ULA) and  $N_{\text{RF}}$  RF chains, where the hybrid precoding architecture is employed and  $N_{\text{RF}} \leq N$  is satisfied. The BS aims to simultaneously serve  $K$  single-antenna UEs, which requires  $N_{\text{RF}} \geq K$ . For analysis simplicity,  $N_{\text{RF}} = K$  is assumed. The downlink system model is first introduced and the uplink channel can be similarly obtained, which is a transpose according to the reciprocity of TDD assumption [4].

In traditional massive MIMO mmWave systems, the received signal for all  $K$  UEs can be represented as

$$\mathbf{y}^{\text{DL}} = \mathbf{H}\mathbf{F}_A\mathbf{F}_D\mathbf{s} + \mathbf{n}, \quad (1)$$

where  $\mathbf{y}^{\text{DL}} = [y_1, y_2, \dots, y_K]^T$  denotes the  $K \times 1$  received signals for all UEs,  $\mathbf{H} = [\mathbf{h}_1, \mathbf{h}_2, \dots, \mathbf{h}_K]^H$  denotes the downlink channel,  $\mathbf{h}_k$  denotes the channel vector between BS and the  $k^{\text{th}}$  UE. The signal vector  $\mathbf{s}$  satisfying the power constraint  $\mathbb{E}[\mathbf{s}\mathbf{s}^H] = \mathbf{I}$  is transmitted to all UEs. The precoding matrices contain two components, i.e., digital precoder  $\mathbf{F}_D$  and analog precoder  $\mathbf{F}_A$ . Finally,  $\mathbf{n} \sim \mathcal{CN}(0, \sigma_n^2 \mathbf{I})$  denotes the Gaussian noise, where  $\sigma_n^2$  denotes the variance of the noise.

The system spectrum efficiency could be expressed as

$$R = \sum_k R_k = \sum_k \log_2 \left( 1 + \frac{p_k |\mathbf{h}_k^H \mathbf{F}_A \mathbf{f}_{D,k}|^2}{\sigma_n^2 + \sum_{l \neq k} p_l |\mathbf{h}_k^H \mathbf{F}_A \mathbf{f}_{D,l}|^2} \right), \quad (2)$$

where  $p_k$  denotes the power allocated to the  $k^{\text{th}}$  UE,  $\mathbf{f}_{D,k}$  denotes the  $k^{\text{th}}$  column of digital precoder  $\mathbf{F}_D$ .

### B. Far-Field Channel Model

The wireless channel can be constructed by either far-field [3] or near-field model [8], where the commonly adopted boundary is Rayleigh distance  $r_{\text{RD}} = \frac{2D^2}{\lambda}$ , where  $D$  and  $\lambda$  denote the array aperture and wavelength, respectively [9]. In 5G massive MIMO communications where the array is not very large, Rayleigh distance is only several meters, meaning that UEs are usually located in the far field, where channels can be modeled by the planar-wave propagation model as

$$\mathbf{h}_k^{\text{far}} = \sqrt{N} \alpha_0 \mathbf{a}(\phi_0) + \sqrt{\frac{N}{L}} \sum_{l=1}^L \alpha_l \mathbf{a}(\phi_l), \quad (3)$$

which contains one line-of-sight (LoS) path and  $L$  non-line-of-sight (NLoS) paths. Parameters  $\alpha_l$  and  $\phi_l$  denote the complex path gain and azimuth angle of the  $l^{\text{th}}$  path, respectively. The index  $l = 0$  represents the LoS path, while  $l \geq 1$  represents the NLoS paths. The channel gains  $\alpha_l$  obey  $\alpha_l \sim \mathcal{CN}(0, \sigma_{\alpha,l}^2)$  for each path, where  $\sigma_{\alpha,0}^2 = \frac{\kappa}{\kappa+1}$  for the LoS path and  $\sigma_{\alpha,l}^2 = \frac{1}{\kappa+1}$

for NLoS paths, respectively. The Rician factor  $\kappa$  denotes the power ratio of LoS and NLoS paths. Due to the planar-wave propagation model, the far-field steering vector  $\mathbf{a}(\phi_l)$  for an  $N$ -element ULA can be expressed as

$$\mathbf{a}(\phi) = \frac{1}{\sqrt{N}} \left[ 1, e^{jkd \sin \phi}, \dots, e^{j\frac{2\pi}{\lambda}(N-1)d \sin \phi} \right]^T, \quad (4)$$

where  $k = \frac{2\pi}{\lambda}$  denotes the wavenumber, and  $d$  denotes the spacing of adjacent antenna elements. However, since the number of antenna elements significantly increases in ELAA systems, the Rayleigh distance significantly increases. For instance, the Rayleigh distance for a 1 m-ULA at 30 GHz reaches 200 m, which covers a large proportion of a cell. Therefore, the electromagnetic propagation model has to be based on spherical waves in ELAA systems [6].

### C. Near-Field Channel Model

Based on the spherical-wave propagation model, the near-field channel can be formulated as [8]

$$\mathbf{h}_k^{\text{near}} = \sqrt{N} \alpha_0 \mathbf{b}(r_0, \phi_0) + \sqrt{\frac{N}{L}} \sum_{l=1}^L \alpha_l \mathbf{b}(r_l, \phi_l), \quad (5)$$

where  $\mathbf{b}(r_l, \phi_l)$  denotes the near-field beam focusing vector, which focuses the signal energy at the location  $(r_l, \phi_l)$ . To emphasize the different properties of near-field beams, we term the single-path near-field channel as *beam focusing vector*, which is opposite to the classical *beam steering vector* defined in (4) in the far-field region.

Adopting the point scatter assumption, the near-field beam focusing vector for an  $N$ -element ULA shown in Fig. 1 is written as

$$\mathbf{b}(r, \phi) = \frac{1}{\sqrt{N}} \left[ e^{-jk(r^{(-\tilde{N})}-r)}, \dots, e^{-jk(r^{(\tilde{N})}-r)} \right]^T, \quad (6)$$

where  $r^{(n)}$  denotes the distance between the scatterer (or UE) and the  $n^{\text{th}}$  antenna element, and  $r$  denotes the distance between the scatterer (or UE) and the center of the array. The maximum index is defined as  $\tilde{N} = \frac{N-1}{2}$ , and  $N$  is assumed to be odd. The distance term  $r_l^{(n)}$  can be written as

$$\begin{aligned} r_l^{(n)} &= \sqrt{r_l^2 + n^2 d^2 - 2ndr_l \sin \phi_l} \\ &\stackrel{(a)}{\approx} r_l - nd \sin \phi_l + \frac{n^2 d^2}{2r_l} \cos^2 \phi_l, \end{aligned} \quad (7)$$

where approximation (a) is derived by the second-order Taylor series expansion  $\sqrt{1+x} = 1 + \frac{x}{2} - \frac{x^2}{8} + \mathcal{O}(x^3)$ . As shown in [10], second-order expansion is usually accurate enough.

**Remark 1.** When Taylor series expansion only keeps the first-order term as  $\sqrt{1+x} \approx 1 + \frac{x}{2}$ , beam focusing vectors in (6) degenerate to beam steering vectors in (3). In other words, far-field beam steering vector is a special case of near-field beam focusing vector without higher-order information.

To sum up, different from far-field channels based on planar-wave assumptions in (4), the phase term based on (7) is related to both spatial angle and distance. Therefore, the

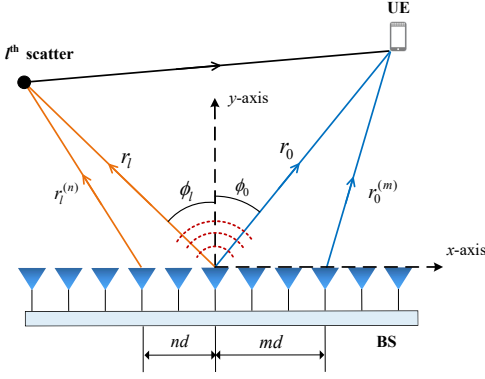


Fig. 1. Near-field channel model for ULA communication systems.

near-field channels for UEs located at the same angle but at different distances are remarkably different. The UEs can be distinguished according to their spatial angle and distance, i.e., their location in the two-dimensional (2D) space, which is a fundamental change compared with far-field communications. In the following section, this extra resolution of near-field beams in the distance domain will be discussed.

### III. ANALYSIS OF ASYMPTOTIC ORTHOGONALITY OF NEAR-FIELD BEAM FOCUSING VECTORS

The correlation of classical far-field steering vectors focusing on  $\phi_l$  and  $\phi_m$  can be formulated as

$$\begin{aligned} |\mathbf{a}^H(\phi_l)\mathbf{a}(\phi_m)| &= \frac{1}{N} \left| \sum_{n=-\tilde{N}}^{\tilde{N}} e^{jnk d(\sin \phi_m - \sin \phi_l)} \right| \\ &= \frac{1}{N} |\Xi_N(kd(\sin \phi_m - \sin \phi_l))|, \end{aligned} \quad (8)$$

where  $\Xi_N(\alpha) = \sin \frac{N\pi}{2}\alpha / (N \sin \frac{\pi}{2}\alpha)$  is the Dirichlet sinc function. According to (8), the correlation of steering vectors achieves the maximum when  $\phi_l = \phi_m$ . If we consider two single-path UEs located at the same angle, the correlation of their channels achieves the maximum and simultaneous transmissions can not be established through precoding. Otherwise, the correlation of steering vectors focusing on different angles tends to be orthogonal with infinite antennas as [4]

$$\lim_{N \rightarrow +\infty} |\mathbf{a}^H(\phi_l)\mathbf{a}(\phi_m)| = 0, \quad \phi_l \neq \phi_m. \quad (9)$$

Therefore, the spatial angular resolution of BS tends to infinity as the number of antennas increases. Owing to the angular orthogonality, BS could distinguish different channel components and multiplex different data streams to different UEs. Therefore, the angular orthogonality of the far-field beam steering vectors contributes to the SDMA scheme [4].

Similarly, we wish to analyze the correlation of near-field beam focusing vectors defined in (6). The correlation of two beam focusing vectors corresponding to the location of  $(r_l, \phi_l)$  and  $(r_m, \phi_m)$  is written as  $|\mathbf{b}^H(r_l, \phi_l)\mathbf{b}(r_m, \phi_m)|$ . According to **Lemma 1** in [8], the correlation of near-field beam focusing vectors corresponding to the same angle but different distances can be illustrated with the following lemma.

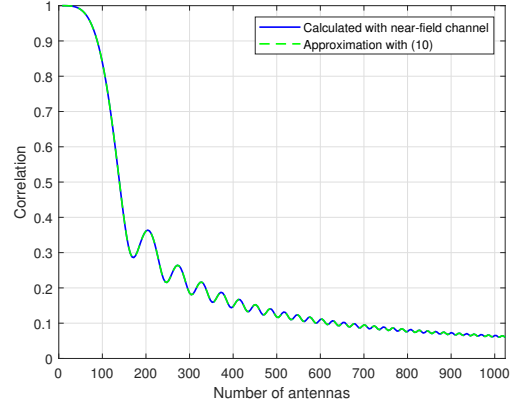


Fig. 2. Correlation of beam focusing vectors with increasing antennas. The frequency is set to 30 GHz and the antennas are half-wavelength spaced.

**Lemma 1.** The correlation of near-field beam focusing vectors corresponding to different distances can be approximated as

$$|\mathbf{b}^H(r_l, \phi)\mathbf{b}(r_m, \phi)| \approx |G(\beta)| = \left| \frac{C(\beta) + jS(\beta)}{\beta} \right|, \quad (10)$$

where  $\beta = N\sqrt{\frac{d^2 \cos^2 \phi}{2\lambda} \left| \frac{1}{r_l} - \frac{1}{r_m} \right|}$ ,  $C(\cdot)$  and  $S(\cdot)$  denote the Fresnel functions written as  $C(x) = \int_0^x \cos(\frac{\pi}{2}t^2)dt$  and  $S(x) = \int_0^x \sin(\frac{\pi}{2}t^2)dt$  [9].

This lemma reveals that the correlation of near-field beam focusing vectors varies with the distance, which fundamentally differs from far-field regions where the correlation of two far-field beam steering vectors is invariable over different distances. We show that the correlation tends to zero as the number of antennas scales up as follows.

**Corollary 1** (Asymptotic Orthogonality in Distance Domain). Near-field beam focusing vectors corresponding to the same angle and different distances are asymptotically orthogonal with the increasing number of antennas, which is to say

$$\lim_{N \rightarrow +\infty} |\mathbf{b}^H(r_l, \phi)\mathbf{b}(r_m, \phi)| = 0, \quad \text{for } r_l \neq r_m. \quad (11)$$

*Proof.* As shown in (10), when the number of antennas  $N$  tends to infinity, the numerator  $C(\beta) + jS(\beta)$  converges to  $0.5 + 0.5j$  and the denominator  $\beta$  tends to  $+\infty$  [9]. Therefore, the correlation converges to 0, which proves the asymptotic orthogonality of beam focusing vectors. ■

To verify the orthogonality in the distance domain, the correlation of beam focusing vectors corresponding to  $(5 \text{ m}, \pi/6)$  and  $(15 \text{ m}, \pi/6)$  is plotted in Fig. 2. It is shown that the correlation significantly decreases as the number of antennas increases. Moreover, (10) can well approximate the accurate correlation. Furthermore, we prove a more general 2D asymptotic orthogonality in both angular and distance domains with the following corollary.

**Corollary 2** (Asymptotic Orthogonality in 2D Domain). Near-field beam focusing vectors corresponding to any different

angles or different distances are also asymptotically orthogonal with the increasing number of antennas, which is to say

$$\lim_{N \rightarrow +\infty} |\mathbf{b}^H(r_l, \phi_l) \mathbf{b}(r_m, \phi_m)| = 0, \text{ for } r_l \neq r_m \text{ or } \phi_l \neq \phi_m. \quad (12)$$

*Proof.* The proof can be seen in [11] Appendix B. ■

The corollary reveals that the angular orthogonality in the far-field region generalizes into the 2D orthogonality in the near-field region, which indicates a stronger potential to establish simultaneous transmissions through precoding in ELAA communications. Therefore, it brings possibilities for a novel multiple access scheme, which is discussed as follows.

#### IV. NEAR-FIELD LDMA SCHEME

As discussed above, near-field beamforming is capable of focusing the energy on a specific location rather than a specific angle. It indicates that, far-field steering beams can be replaced by near-field focusing beams to distinguish users at different locations and suppress interferences from other UEs in the same direction. Following this intuition, the concept of LDMA is proposed, employing near-field location-dependent beam focusing vectors as analog precoders to serve different UEs located in different locations. Compared with SDMA, the proposed LDMA provides a method to harvest extra orthogonal resources in the distance dimension.

Specifically, the proposed LDMA scheme comprises three main stages, including: Initial access, uplink equivalent channel estimation, and uplink/downlink data transmission. In the initial access procedure, BS could perform beam sweeping to establish a physical link connection to idle UEs. Each UE is scheduled with a specific codeword as the analog precoder  $\mathbf{w}_k$  from a predefined near-field codebook  $\mathcal{W} = [w_1, \dots, w_M]$ . It is worth noting that, the codebook can be designed with constraints on the maximum correlation between different codewords [8]. For fixed correlation, the distance between focal points can be determined by (10) correspondingly, revealing the distance resolution of LDMA. Therefore, by adjusting the correlation of codewords, the distance resolution can be determined. Then, the analog precoding for all connected UEs can be designed as  $\mathbf{F}_A = [\mathbf{w}_1, \mathbf{w}_2, \dots, \mathbf{w}_K]$ . Afterward, BS could estimate the effective channel with uplink pilots as

$$\bar{\mathbf{h}}_k = \mathbf{F}_A^H \mathbf{h}_k + \mathbf{F}_A^H n_k, \quad (13)$$

where  $n_k$  denotes the noise corresponding to the  $k^{\text{th}}$  UE. Finally, the BS could design the digital precoder through the estimated effective channel by weighted minimum mean square error (WMMSE) as in [12] or zero-forcing (ZF) as

$$\mathbf{F}_D = \bar{\mathbf{H}}^H (\bar{\mathbf{H}} \bar{\mathbf{H}}^H)^{-1} \Lambda, \quad (14)$$

where  $\bar{\mathbf{H}} = [\bar{\mathbf{h}}_1, \dots, \bar{\mathbf{h}}_K]^H$  denotes the effective channel of all  $K$  UEs. The diagonal matrix  $\Lambda$  denotes the power allocation for different UEs, which is designed to satisfy  $\|\mathbf{F}_A \mathbf{f}_{D,k}\|^2 = 1$ . Apart from WMMSE and ZF, other design methods are also supported to design digital precoders. To sum up, the LDMA scheme can be summarized in **Algorithm 1**.

---

#### Algorithm 1 Location Division Multiple Access.

---

- Input:** Multi-user channel  $\mathbf{H}$ , near-field codebook  $\mathcal{W}$ .  
**Output:** Digital precoder  $\mathbf{F}_D$  and analog precoder  $\mathbf{F}_A$
- 1: **Initial Access:**
  - 2: BS performs beam sweeping with  $\mathcal{W}$  and each UE reports the beam decision to BS;
  - 3: BS selects the best codeword  $\mathbf{w}_k$  for  $k^{\text{th}}$  UE from  $\mathcal{W}$  and construct the analog precoder  $\mathbf{F}_A = [\mathbf{w}_1, \mathbf{w}_2, \dots, \mathbf{w}_K]$ ;
  - 4: **Uplink Equivalent Channel Estimation:**
  - 5: Each UE sends uplink non-orthogonal pilots;
  - 6: BS estimates the effective channel  $\bar{\mathbf{h}}_k$  by (13);
  - 7: BS designs digital combiner and precoder  $\mathbf{F}_D$  by (14);
  - 8: **Uplink/Downlink Data Transmission:**
  - 9: BS performs combining/precoding with  $\mathbf{F}_D$  and  $\mathbf{F}_A$ ;
  - 10: **return** Digital precoder  $\mathbf{F}_D$  and analog precoder  $\mathbf{F}_A$ .
- 

#### V. PERFORMANCE ANALYSIS

##### A. Asymptotic Spectrum Efficiency for Single-path Channels

To investigate the system performance of LDMA, we first assume a single-path channel scenario. The single-path channel could be written as  $\mathbf{h}_k = \sqrt{N} \alpha_k \mathbf{b}(r_k, \phi_k)$ . If BS acquires the perfect channel state information, the optimal analog precoder for all  $K$  UEs can be written as  $\mathbf{F}_A = \mathbf{B} = [\mathbf{b}(r_1, \phi_1), \dots, \mathbf{b}(r_K, \phi_K)]$ . For analysis simplicity, the ZF-based digital precoder is adopted. In addition, the large-scale fading is neglected by employing reasonable power control and thus different UEs share the same channel gain. The spectrum efficiency can be obtained by the following lemma.

**Lemma 2.** With equal power allocation for different UEs, the spectrum efficiency achieved by **Algorithm 1** is given by

$$R = \sum_{k=1}^K \log_2 \left( 1 + \frac{P}{K \sigma_n^2} \frac{N |\alpha_k|^2}{[\mathbf{B}^H \mathbf{B}]_{k,k}^{-1}} \right), \quad (15)$$

where  $P$  denotes the total transmission power,  $[\mathbf{B}^H \mathbf{B}]_{k,k}^{-1}$  denotes the  $k^{\text{th}}$  diagonal entry of the matrix  $(\mathbf{B}^H \mathbf{B})^{-1}$ .

*Proof.* The proof can be seen in [11] Appendix C. ■

For multi-user MIMO systems, an ideal communication scenario is that multiple UEs could be served by BS without interferences, leading to the ideal spectrum efficiency as

$$\hat{R} = \sum_{k=1}^K \log_2 \left( 1 + \frac{P}{K \sigma^2} N |\alpha_k|^2 \right). \quad (16)$$

Due to the asymptotic orthogonality proved in **Corollary 2**, the spectrum efficiency could approach the ideal one according to the following corollary.

**Corollary 3.** If the number of BS antennas  $N$  tends to infinity, the spectrum efficiency for a fixed number of UEs approaches the ideal spectrum efficiency with probability one, i.e.,

$$\mathbb{P} \left[ \lim_{N \rightarrow +\infty} R = \hat{R} \right] = 1. \quad (17)$$

*Proof.* The proof can be seen in [11] Appendix D. ■

Therefore, as the number of antennas tends to infinity, the asymptotic optimality could be ensured for LDMA schemes.

### B. Linear Distribution Analysis

Compared with SDMA, the ability to serve single-path UEs residing in the same angle could be viewed as a feature distinguishing LDMA from SDMA. To verify this advantage, we consider a special scenario where UEs are linearly distributed.

First, we consider a simple three UEs system, where UEs are distributed in a certain direction  $\phi$  and distance range of  $[r_{\min}, r_{\max}]$ . Without loss of generality, we assume  $r_1 \leq r_2 \leq r_3$ . According to **Lemma 2**, the analog precoder can be obtained as  $\mathbf{B}_{\text{TU}} = [\mathbf{b}(r_1, \phi), \mathbf{b}(r_2, \phi), \mathbf{b}(r_3, \phi)]$ . The maximum spectrum efficiency of this system can be obtained based on the following assumptions:

- (i) Single-path channel is adopted and high SNR is assumed.
- (ii) Interferences of non-adjacent UEs are neglected, i.e. the interference of 1<sup>st</sup> and 3<sup>rd</sup> UE is approximated by 0.
- (iii) ZF-based digital precoders are adopted.

Then, we can denote  $\mathbf{B}_{\text{TU}}^H \mathbf{B}_{\text{TU}}$  as

$$\mathbf{T}_{\text{TU}} = \mathbf{B}_{\text{TU}}^H \mathbf{B}_{\text{TU}} = \begin{bmatrix} 1 & \delta_{21}^* & 0 \\ \delta_{21} & 1 & \delta_{32}^* \\ 0 & \delta_{32} & 1 \end{bmatrix}, \quad (18)$$

where  $\delta_{ij} = \mathbf{b}^H(r_i, \phi) \mathbf{b}(r_j, \phi)$  denotes the product of the  $i^{\text{th}}$  and  $j^{\text{th}}$  beam focusing vector. Suppose the locations of the first and third UE are fixed, the maximum achievable spectrum efficiency could be approximated by the following lemma.

**Lemma 3.** We assume  $\delta_{21} = g(x)$  and  $\delta_{32} = g(r_0 - x)$ , where  $g(x)$  is defined as  $g(x) : \mathbb{R}_+ \rightarrow \mathbb{C}$ , and  $|g(x)|^2$  is monotonically decreasing and convex, satisfying  $0 \leq |g(x)| \leq 1$  and  $r_0 > 0$ . The spectrum efficiency with  $\mathbf{T}_{\text{TU}}$  satisfies

$$R_{\text{TU}}(x) \lesssim R(x)^{\text{aub}} = 2 \log_2 \left( 1 + \frac{P}{K\sigma_n^2} \frac{N|\alpha|^2(1-2g(\hat{x}))}{(1-g(\hat{x}))} \right) + \log_2 \left( 1 + \frac{P}{K\sigma_n^2} N|\alpha|^2(1-2g(\hat{x})) \right). \quad (19)$$

The equality holds when  $x = \hat{x}$  satisfying  $g(\hat{x}) = g(r_0 - \hat{x})$ .

*Proof.* The proof can be seen in [11] Appendix E. ■

**Remark 2.** It can be proved that the envelope of  $|G(\beta)|$  in (10) approximately satisfies the monotonically decreasing and convex property. Therefore, the maximum spectrum efficiency can be approximately obtained through **Lemma 3** for a three-UE system. It is worth noting that, this conclusion is drawn under the assumption that interference from non-adjacent UEs is neglected. Therefore, this lemma can be viewed as an approximated upper bound for real communication scenarios.

Under the same three assumptions, the conclusion of **Lemma 3** can be generalized into multi-user scenarios. Specifically, we consider a system where multiple UEs are linearly distributed. If we investigate any adjacent three UEs, the middle UE must be located in the position according to **Lemma 3**.

Then, the maximum spectrum efficiency of linearly distributed UEs can be obtained through the following lemma.

**Lemma 4.** The approximated upper bound of the spectrum efficiency of linearly distributed UEs can be expressed as

$$R_K \lesssim R^{\text{aub}} = \sum_{k=1}^K \log_2 \left( 1 + \frac{P}{K\sigma_n^2} \frac{N|\alpha_k|^2}{\gamma_k} \right), \quad (20)$$

where  $\gamma_k$  is determined by

$$\gamma_k = \frac{(\chi_1 x_1^{k-2} + \chi_2 x_2^{k-2})(\chi_1 x_1^{K-k-1} + \chi_2 x_2^{K-k-1})}{\chi_1 x_1^{K-1} + \chi_2 x_2^{K-1}}, \quad (21)$$

and  $x_1, x_2$  are solutions to  $x^2 - x + |\delta|^2 = 0$ , and  $\chi_1 = -\frac{x_1^2}{x_2 - x_1}$ ,  $\chi_2 = \frac{x_2^2}{x_2 - x_1}$ ,  $|\delta|$  is defined as the min-max correlation between UEs as  $|\delta| = \min_{r_1, \dots, r_K} \max_{i \neq j} |\mathbf{b}^H(r_i, \phi) \mathbf{b}(r_j, \phi)|$ .

*Proof.* The proof can be seen in [11] Appendix F. ■

## VI. SIMULATION RESULTS

### A. Linear Distribution Scenarios

We first consider a linear distribution scenario, where UEs are aligned along the spatial angle  $\phi = 0$ . Each UE is located within the range  $[4 \text{ m}, 150 \text{ m}]$ . The number of UEs varies in  $[1, 14]$  and SNR is set to be 12 dB. The frequency is 30 GHz and the array is half-wavelength spaced 256-element ULA with  $d = \lambda/2 = 0.5 \text{ cm}$ .

The spectrum efficiency with increasing number of UEs is plotted in Fig. 3. The red line and blue line represent the situation where UEs are placed to minimize the interference from adjacent UEs without and with non-adjacent (NA) interference, respectively. The red line denotes the approximated upper bound derived in (20) neglecting the NA interference, which is unreachable. A reachable spectrum efficiency for the same UE position is plotted in blue. An exhaustive search is performed to search for the realistic maximum spectrum efficiency by changing the position of UEs, which is plotted in green. It shows that the approximated upper bound in (20) is very tight for small number of UEs and provides an approximately ideal distribution of UEs. Therefore, **Lemma 3** provides accurate estimations of maximum spectrum efficiency.

In addition, the orange line represents randomly and linearly distributed UEs and the black dashed line denotes the spectrum efficiency employing far-field SDMA where only one UE could access to the BS since channels for all UEs are constructed based on the same steering vector. It shows that even randomly distributed UEs with LDMA also outperforms far-field SDMA when the number of UEs is not very large.

Then, we consider a multi-path model where both LoS and NLoS paths exist. The UEs are located within the range of  $[4 \text{ m}, 100 \text{ m}]$ . The number of UEs is  $K = 4$  and the number of NLoS paths is  $L = 5$ . The near-field polar-domain codebook in [8] is adopted and the far-field DFT codebook is adopted as the classical far-field SDMA baseline [5]. Both ZF and WMMSE are considered for designing digital precoders. The simulation result is shown in Fig. 4. The

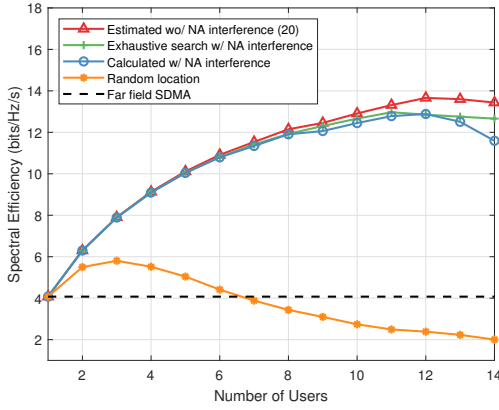


Fig. 3. Verification of the approximated upper bound of the spectrum efficiency for linear distributed UEs.

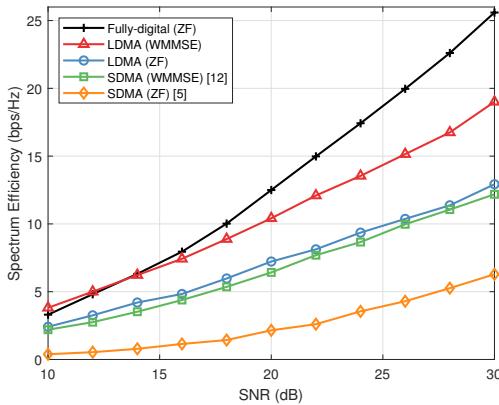


Fig. 4. Comparison of the proposed LDMA and classical far-field multiple access under the linear distribution assumption.

proposed LDMA outperforms SDMA on both WMMSE and ZF scenarios, with about 60% and 240% performance gain compared with WMMSE- and ZF-based SDMA at SNR = 20 dB, respectively. In addition, the proposed WMMSE-based LDMA outperform the ZF-based fully-digital precoding in low SNR scenarios since ZF enlarges the noise. In high SNR scenarios, WMMSE-based LDMA could approach the ideal fully-digital precoding.

#### B. Uniform Distribution Scenarios

Next, we consider a more general scenario where UEs are uniformly distributed within the cell, with a radius range [4 m, 100 m] and angle range  $[-\pi/3, \pi/3]$ . The number of NLoS paths and UEs are set to  $L = 5$  and  $K = 10$ . Both ZF and WMMSE are adopted for designing digital precoders. Simulation results are shown in Fig. 5. The WMMSE-based LDMA scheme achieves nearly 100% improvement at SNR = 20 dB compared with WMMSE-based SDMA. Also, since the near-field precoding could be leveraged to manage inter-user interference, the performance gap between proposed LDMA with far-field SDMA increases as SNR increases.

### VII. CONCLUSIONS

In this paper, the concept of LDMA is first proposed, which leverages the near-field beam focusing property to mitigate

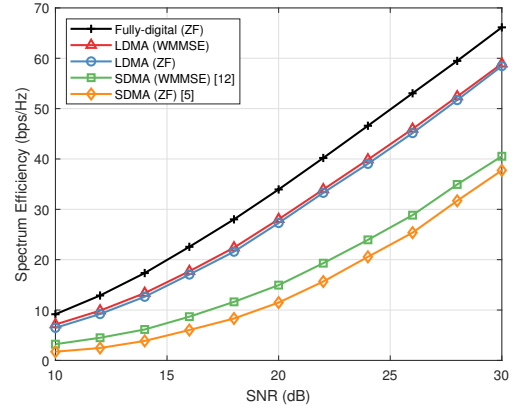


Fig. 5. Comparison of the proposed LDMA and classical SDMA under the uniform distribution assumption.

interferences and significantly enhance spectrum efficiency. Similar to the asymptotic angular orthogonality of far-field beams, the asymptotic orthogonality of near-field beams in the distance domain is proved and the LDMA scheme is investigated. Simulation results verify the superiority of the proposed LDMA scheme over uniform and linear distribution scenarios. We hope the LDMA scheme could provide a new possibility for spectrum efficiency enhancement compared classical SDMA for the widely adopted hybrid precoding.

### REFERENCES

- [1] T. L. Marzetta, "Noncooperative cellular wireless with unlimited numbers of base station antennas," *IEEE Trans. Wireless Commun.*, vol. 9, no. 11, pp. 3590–3600, Oct. 2010.
- [2] L. Sanguinetti, E. Björnson, and J. Hoydis, "Toward massive MIMO 2.0: Understanding spatial correlation, interference suppression, and pilot contamination," *IEEE Trans. Commun.*, vol. 68, no. 1, pp. 232–257, Jan. 2020.
- [3] O. Ayach, S. Rajagopal, S. Abu-Surra, Z. Pi, and R. W. Heath, "Spatially sparse precoding in millimeter wave MIMO systems," *IEEE Trans. Wireless Commun.*, vol. 13, no. 3, pp. 1499–1513, Jan. 2014.
- [4] C. Sun, X. Gao, S. Jin, M. Matthaiou, Z. Ding, and C. Xiao, "Beam division multiple access transmission for massive MIMO communications," *IEEE Trans. Commun.*, vol. 63, no. 6, pp. 2170–2184, Apr. 2015.
- [5] A. Alkhateeb, G. Leus, and R. W. Heath, "Limited feedback hybrid precoding for multi-user millimeter wave systems," *IEEE Trans. Wireless Commun.*, vol. 14, no. 11, pp. 6481–6494, Jul. 2015.
- [6] M. Cui, Z. Wu, Y. Lu, X. Wei, and L. Dai, "Near-field communications for 6G: Fundamentals, challenges, potentials, and future directions," *IEEE Commun. Mag. (early access)*, pp. 1–7, Sep. 2022.
- [7] N. J. Myers and R. W. Heath, "Infocus: A spatial coding technique to mitigate misfocus in near-field LoS beamforming," *IEEE Trans. Wireless Commun.*, vol. 21, no. 4, pp. 2193–2209, Sep. 2022.
- [8] M. Cui and L. Dai, "Channel estimation for extremely large-scale MIMO: Far-field or near-field?" *IEEE Trans. Commun.*, vol. 70, no. 4, pp. 2663–2677, Jan. 2022.
- [9] J. Sherman, "Properties of focused apertures in the fresnel region," *IEEE Trans. Antennas Propag.*, vol. 10, no. 4, pp. 399–408, Jul. 1962.
- [10] K. T. Selvan and R. Janaswamy, "Fraunhofer and fresnel distances: Unified derivation for aperture antennas," *IEEE Antennas Propag. Mag.*, vol. 59, no. 4, pp. 12–15, Jun. 2017.
- [11] Z. Wu and L. Dai, "Multiple access for near-field communications: SDMA or LDMA?" *arXiv preprint arXiv:2208.06349*, Oct. 2022.
- [12] Q. Shi, M. Razaviyayn, Z.-Q. Luo, and C. He, "An iteratively weighted MMSE approach to distributed sum-utility maximization for a MIMO interfering broadcast channel," *IEEE Trans. Signal Process.*, vol. 59, no. 9, pp. 4331–4340, Apr. 2011.